Thermodynamic and Kinetic Destabilization in LiBH$_4$/Mg$_2$NiH$_4$: Promise for Borohydride-Based Hydrogen Storage

John J. Vajo*, Wen Li , and Ping Liu

Supporting Information

5

1. Experimental details
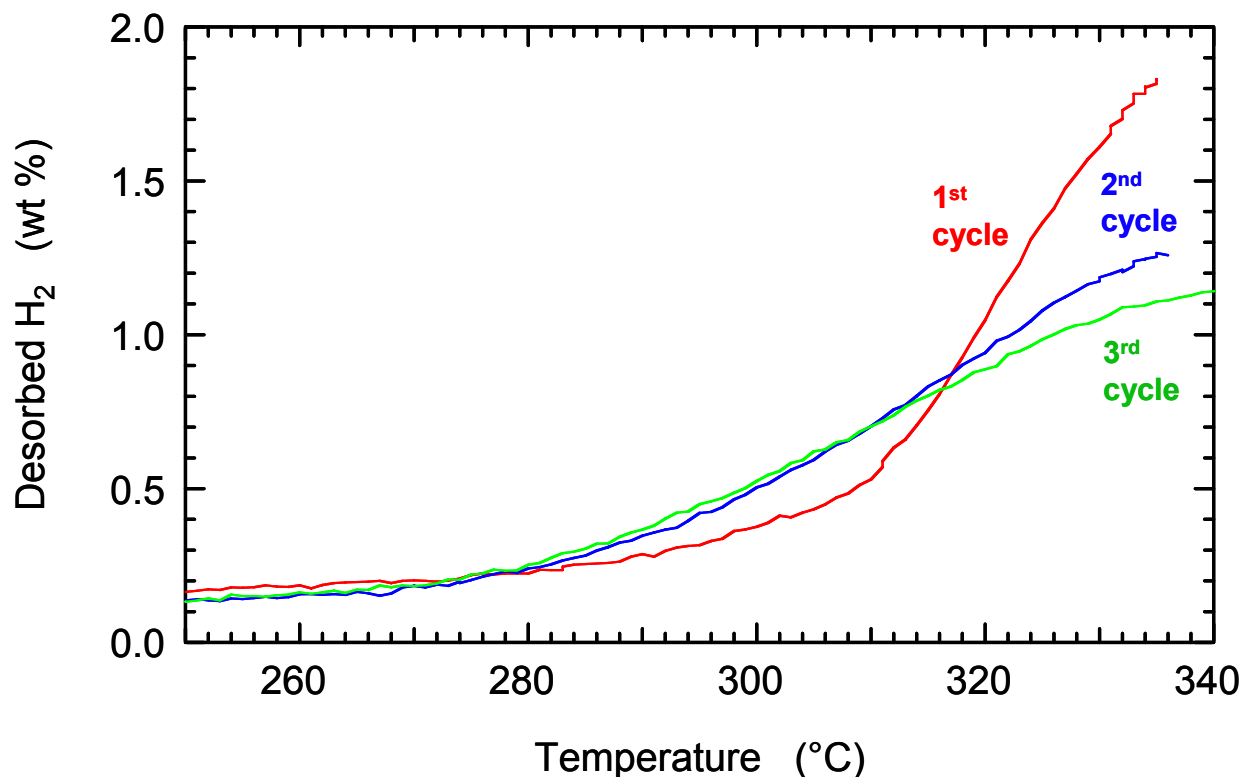
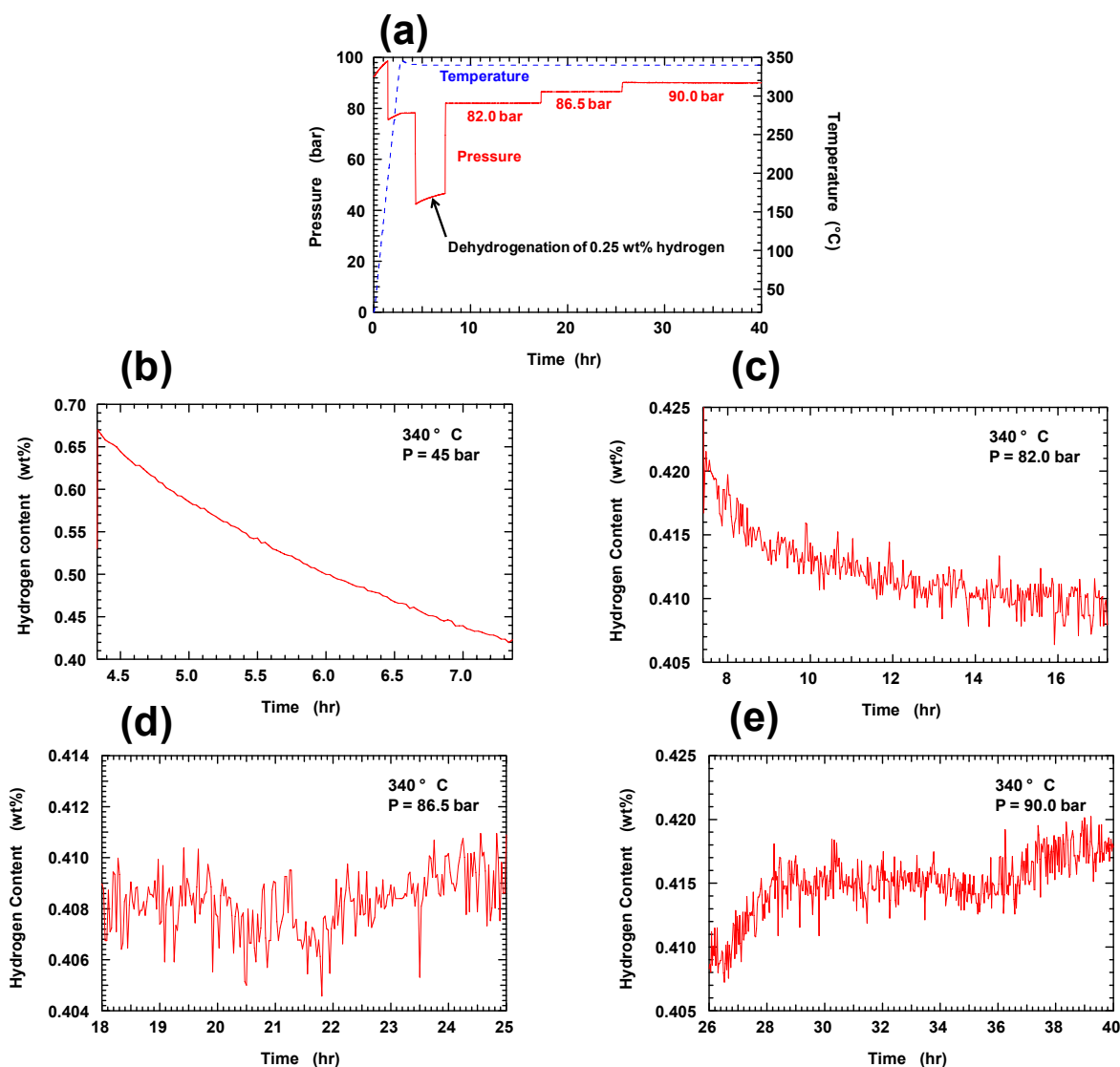All sample handling was performed in an argon-filled glove box with < 1 ppm H$_2$O and O$_2$ concentrations.

Lithium borohydride from Aldrich, ≥ 90% purity, was used without further purification. Magnesium nickel hydride (nominal stoichiometry of Mg$_2$NiH$_4$) was prepared from a Mg$_2$Ni alloy (HY-STOR alloy 301, Ergenics). This alloy has an

10 actual composition of Mg$_{2.35}$Ni. The alloy was hydrogenated in 100 bar H$_2$ at 350 °C and then dehydrogenated and rehydrogenated twice to insure maximum hydrogenation. Based on the alloy composition, the actual composition of the hydrogenated product was Mg$_2$NiH$_4$ + 0.35MgH$_2$. However, mixtures of LiBH$_4$ and Mg$_2$NiH$_4$ with an intended ratio of 4LiBH$_4$: 5Mg$_2$NiH$_4$ were prepared using the nominal (Mg$_2$NiH$_4$) composition. Given the excess MgH$_2$, the actual stoichiometry of the mixture was, therefore, rich in LiBH$_4$ with a ratio of 4.33LiBH$_4$: 5Mg$_2$NiH$_4$.

15 The mixtures were mechanically milled using a Fritsch Pulversette 6 planetary mill. Approximately 1.2 g of the mixtures were loaded into an 80 cm^3 hardened steel vessel with 30 chrome-steel balls 7 mm in diameter. The vessel was sealed under argon in the glove box with an elastomeric gasket and milled at 400 rpm for 1 hr.

X-ray data were obtained with a Philips PW3040/60 X'Pert Pro diffractometer using Cu Kα radiation with a combination of an X-ray mirror and a 2-crystal Ge(220) 4-bounce monochrometer. Samples were mounted into 1 mm glass capillary

20 tubes in the glove box and sealed prior to data acquisition. A broad feature seen the X-ray diffraction patterns at 15 – 60° two-theta originates from the glass walls of the capillary tubes.
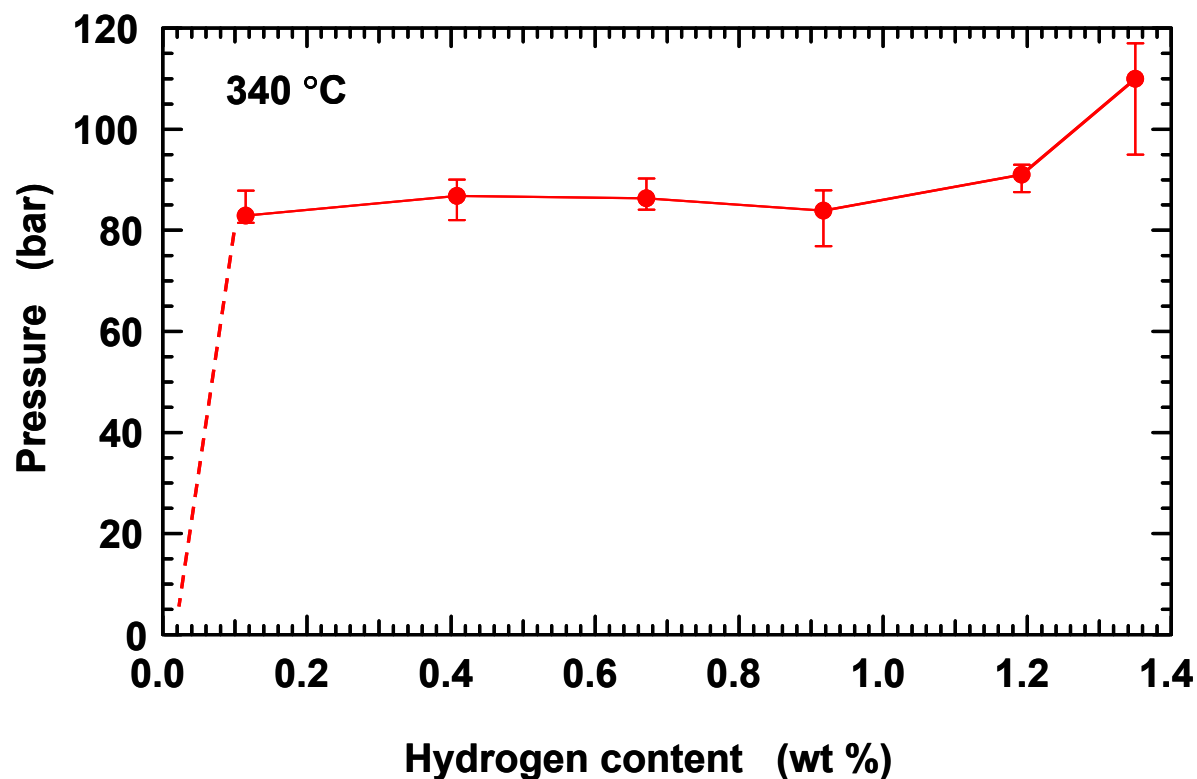
2. SFig. 1. Cycling of $4LiBH_4 + 5Mg_2NiH_4$. Desorption data for the 1st reaction step are shown for three cycles as a function of temperature during heating at 2 °C/min. In the figure, the data shown were cut off after the first step, ~336 °C, although the temperature ramp continued until 450 °C. After the first and second cycles, the sample was rehydrogenated by heating in 100 bar H_2 at 350 °C for 2 hr and then 300 °C for 2 hr. The capacity decreases from the first to the second cycle but then stabilizes while the kinetics improve at low temperatures. For this work the reversible capacity of the 1st reaction step was 1.35 wt%, which is only ~50% of the theoretical capacity. Some of the discrepancy is due to the excess $LiBH_4$ as described in the Experimental Details. However, the reversible capacity also seems to be limited by the kinetics. While longer reaction times did not improve the capacity, longer milling times, up to 48 hr, increased the reversible capacity up to 1.7 wt%.
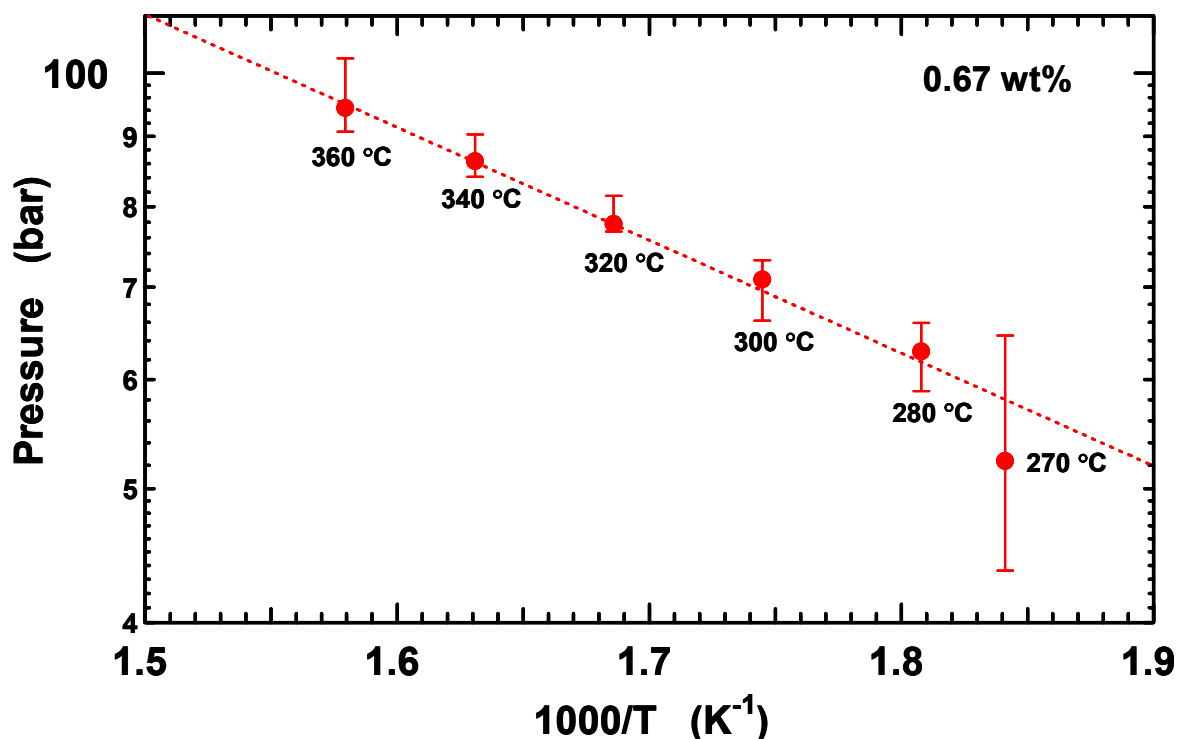
3. SFig. 2. Measurement of equilibrium pressures for the 1st reaction step. Shown in SFig. 2a. is a portion of the raw data (system pressure and sample temperature vs. time) used to determine the equilibrium pressures shown in Figure 3 and SFig. 4, and the isotherm shown in SFig. 3. The step function changes in pressure are due to the addition or removal of hydrogen from the sample volume. The gradual changes in pressure are due to heating or changes in the hydrogen content of the sample. This portion of the data begins at an absolute hydrogen content of 0.67 wt%. The sample was heated to 340 °C during the first 3 hr in ~85 bar hydrogen. At 4 hr, the pressure was lowered to 45 bar to desorb hydrogen at a relatively fast rate. During the next 3 hr, desorption of 0.25 wt% hydrogen occurred as noted in the figure. After quantification to yield absolute hydrogen content, this portion of the data is shown in SFig. 2b. This desorption step brought the absolute hydrogen content to 0.67-0.25 = 0.42 wt%. At this point the equilibrium pressure was determined by adjusting the pressure until a small rate of dehydrogenation was detectable. Then, the pressure was increased until a small rate of hydrogenation occurred. In the figure, this is shown in three pressure steps. In the first step, the pressure was increased to 82.0 bar. At this pressure there was a slow desorption as shown (after quantification to show absolute hydrogen content) in SFig. 2c. A simple linear fit over the whole interval shown gave a hydrogenation rate of -0.000803 wt%/hr (note, the sample was actually dehydrogenating, so the hydrogenation rate is negative). The sample mass and the sorption volume were chosen
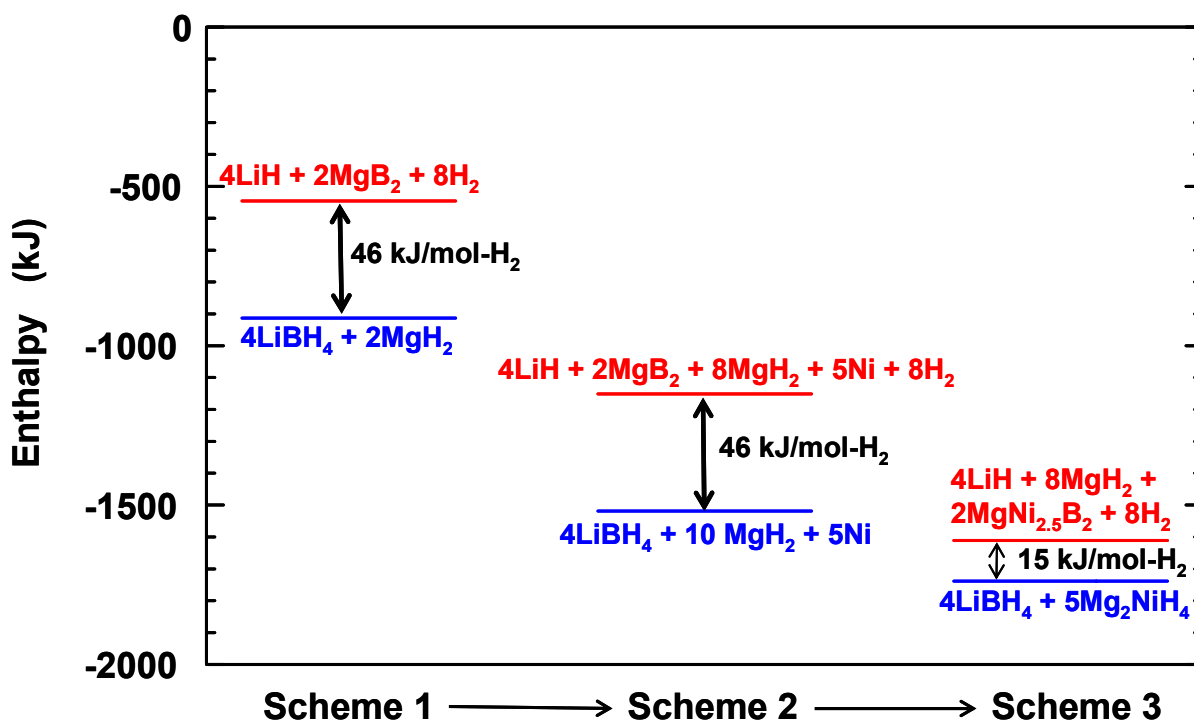
such that negligible change in the hydrogen content or the pressure occurred. For example, during the interval at 82.0 bar, the hydrogen content changed by ~0.01 wt%. In the second step, the pressure was increased to 86.5 bar. This pressure is very close to equilibrium as shown in SFig. 2d (again, quantified to show absolute hydrogen content). A linear fit indicated that hydrogenation was occurring, at a rate of 0.000212 wt%/hr. In the third step, the pressure was increased to 90.0 bar.

5 At this pressure, as shown in SFig. 2e after quantification to give absolute hydrogen content, hydrogenation was clearly occurring.   A linear fit gave a hydrogenation rate of 0.000353 wt%/hr. Again, the change in the hydrogen content was ~0.01 wt%. From these data, the equilibrium pressure was estimated by assuming a linear dependence of the hydrogenation rate on pressure and determining the pressure at which the rate equals zero. (Ref. S1) From these data, the equilibrium pressure was estimated to be 86.8 bar. This data point (86.8 bar at 0.42 wt%) is plotted in the isotherm shown

10 in SFig. 3. We note that because the pressures at which the hydrogenation and dehydrogenation rates were measured closely bracketed the equilibrium pressure, the assumption of a linear dependence of the sorption rate on pressure is not critical. In fact, simply averaging the pressures at which hydrogenation and dehydrogenation were clearly observed gave similar values for the equilibrium pressures. We found that using this method to determine equilibrium pressures avoids the long equilibration times and subjectivity in conventional measurements in which an asymptotic pressure is measured, or

15 estimated by extrapolation, following dosing with hydrogen. (Ref. S2) This method also gives an estimate of equilibrium pressures without hysteresis originating from the reaction direction and is particularly applicable to multiple phase systems that are expected to display flat isotherms with little intrinsic hysteresis. This method does require a relatively large sample mass and a relatively small sorption volume to insure that hydrogenation and dehydrogenation can be measured under conditions where the pressure change and change in hydrogen content are negligible. In this work, these requirements were

20 achieved by using a sample mass of ~3.6 g and a sorption volume of ~30 cm^3.

Supplementary Material (ESI) for Chemical Communications
This journal is (c) The Royal Society of Chemistry 2010
www.rsc.org/chemcomm | ChemComm

4. SFig. 3. Equilibrium isotherm for LiBH$_4$/Mg$_2$NiH$_4$ reaction at 340 °C. Equilibrium pressures were determined at 340 °C using the procedure described in SFig. 2. The reversible capacity was 1.35 wt%. The error bars originate from the closest pressures where hydrogenation (for positive error bars) and dehydrogenation (for the negative error bars) were measured, as described in SFig. 2. Within the experimental uncertainties, the isotherm is flat from ~ 0.1 to 1 wt% hydrogen. This isotherm was measured over several complete hydrogenation/dehydrogenation cycles with the points at 0.4 and 1.2 wt% measured last. The consistency of the data indicates that the cycling is reproducible with no significant changes over ~10 cycles.

5. SFig. 4. Van't Hoff plot for LiBH$_4$/Mg$_2$NiH$_4$ reaction at 0.67 wt% hydrogen content. Using the technique described in SFig. 2, the temperature dependence of the equilibrium pressure was measured at a hydrogen content of 0.67 wt%. When

5 changing the temperature, appropriate changes in the hydrogen pressure were also made to maintain constant hydrogen content. However, full isotherms were not measured at temperatures other than 340 °C. This method follows the "Direct van't Hoff" method developed at Hy-Energy. (Ref. S3) The error bars shown originate from the closest pressures where hydrogenation (for positive error bars) and dehydrogenation (for the negative error bars) were clearly measured, as described in SFig. 2. The error bars for the lowest temperature data point (at 270 °C) are particularly large because, at this

10 temperature, larger deviations from equilibrium were needed to obtain measurable sorption rates. These data together with the isotherm in SFig. 3 were collected over ~10 complete hydrogenation/dehydrogenation cycles with the data point at 320 °C measured last. Thus, the linear behaviour is reproducible. A linear fit to the data using the error bars as uncertainties give an enthalpy, $\Delta H = 15.4 \pm 2$ kJ/mol-H$_2$, an entropy $\Delta S = 62.2 \pm 3$ J/K-mol-H$_2$, and a temperature for 1 bar equilibrium pressure, $T_{1bar} = -25$ °C. The data point at 270 °C is below the trend established at higher temperatures, which could

15 indicate a change in enthalpy commensurate with the solidification of LiBH$_4$ at ~285 °C. However, the experimental uncertainties at 270 °C are large and, thus, further measurements are needed to explore this possibility.

6. SFig. 5. Enthalpy diagram. To understand the enthalpy change in the $LiBH_4/Mg_2NiH_4$ system, an enthalpy diagram was constructed beginning from the $LiBH_4/MgH_2$ system. The following standard formation enthalpies (ΔH_f), obtained from the HSC database (Ref. S4) were used:

ΔH_f ($LiBH_4$) = -190.5 kJ/mol

ΔH_f (LiH) = -90.5 kJ/mol

ΔH_f (MgH_2) = -75.5 kJ/mol

ΔH_f (MgB_2) = -92.0 kJ/mol

ΔH_f (Mg_2Ni) = -66.9 kJ/mol

An enthalpy for the dehydrogenation of Mg_2NiH_4 of 64.5 kJ/mol-H_2 was used to obtain:

ΔH_f (Mg_2NiH_4) = -196 kJ/mol.

From these values, the three reaction schemes shown were constructed. In each case the low enthalpy state (in blue) is the hydrogenated state and the high enthalpy state (in red) is dehydrogenated state. Scheme 1 is the $LiBH_4/MgH_2$ reaction. Based on standard formation enthalpies, which do not include solid-solid phase transitions or melting, this reaction has an enthalpy change of 46 kJ/mol-H_2. In Scheme 2, 8 moles of MgH_2 and 5 moles of Ni have been added to both the hydrogenated and the dehydrogenated states. Because there is no overall chemical change from Scheme 1 to Scheme 2, the enthalpy change is unaffected. Scheme 3 is the $LiBH_4/Mg_2NiH_4$ reaction. This reaction was obtained from Scheme 2 by forming $5Mg_2NiH_4$ in the hydrogenated state (from $8MgH_2 + 5Ni$) and $2MgNi_{2.5}B_2$ in the dehydrogenated state (from

$2MgB_2 + 5Ni$). To our knowledge there is no measurement of the standard formation enthalpy for $MgNi_{2.5}B_2$, so the absolute enthalpy of the dehydrogenated state was determined from the hydrogenated state using the experimental enthalpy change (15 kJ/mol-H_2). From a comparison of the enthalpy levels going from Scheme 2 to Scheme 3, it can be seen that the small enthalpy change for the $LiBH_4$/Mg_2NiH_4 reaction is largely due to the stability of the $MgNi_{2.5}B_2$ phase. From these calculations we estimate:

$\Delta H_f (MgNi_{2.5}B_2) = $ -323 kJ/mol

On a per atom basis, this ternary boride (-59 kJ/atom) is almost twice as stable as MgB_2 (-31 kJ/atom).

Supporting Information References

Ref. S1. Huot, J. in Nanoclusters and nanocrystals, Nalwa, H. S. (Ed.) American Scientific Publishers, p. 53, 2003.

Ref. S2. Borgschulte, A.; Kato, S.; Bielmann, M.; Zuttel, A. in Proceedings of the International Symposium Materials Issues in a Hydrogen Economy, Jena, P.; Kandalam, A.; Sun, Q. (Eds.) World Scientific, p. 184, 2009.

Ref. S3. See slides 22 – 25 in http://hydrogendoedev.nrel.gov/pdfs/review08/st_3_gross.pdf

Ref. S4. Outokumpu HSC Chemistry, version 4.0; ChemSW, Inc., 1999.